

## Pillared Bentonite Materials as Potential Solid Acid Catalyst for Diethyl Ether Synthesis: A Brief Review

Puji Wahyuningsih<sup>1,2</sup>, Karna Wijaya<sup>1†</sup>, Aulia Sukma Hutama<sup>1</sup>, Aldino Javier Saviola<sup>1</sup>,  
Indra Purnama<sup>3</sup>, Won-Chun Oh<sup>4</sup>, and Muhammad Aziz<sup>5</sup>

<sup>1</sup>Department of Chemistry, Faculty of Mathematics and Natural Sciences, Universitas Gadjah Mada, Yogyakarta 55281, Indonesia

<sup>2</sup>Department of Chemistry, Faculty of Engineering, Universitas Samudra, Aceh 24354, Indonesia

<sup>3</sup>Graduate School of Agricultural Sciences, Universitas Lancang Kuning, Pekanbaru 28261, Indonesia

<sup>4</sup>Department of Advanced Materials and Engineering, Hanseo University, Seosan 31962, Republic of Korea

<sup>5</sup>Institute of Industrial Science, The University of Tokyo, Tokyo 1538505, Japan

(Received February 23, 2024 : Revised May 14, 2024 : Accepted May 15, 2024)

**Abstract** This review explores the potential of pillared bentonite materials as solid acid catalysts for synthesizing diethyl ether, a promising renewable energy source. Diethyl ether offers numerous environmental benefits over fossil fuels, such as lower emissions of nitrogen oxides (NO<sub>x</sub>) and carbon oxides (CO<sub>x</sub>) gases and enhanced fuel properties, like high volatility and low flash point. Generally, the synthesis of diethyl ether employs homogeneous acid catalysts, which pose environmental impacts and operational challenges. This review discusses bentonite, a naturally occurring alumina silicate, as a heterogeneous acid catalyst due to its significant cation exchange capacity, porosity, and ability to undergo modifications such as pillarization. Pillarization involves intercalating polyhydroxy cations into the bentonite structure, enhancing surface area, acidity, and thermal stability. Despite the potential advantages, challenges remain in optimizing the yield and selectivity of diethyl ether production using pillared bentonite. The review highlights the need for further research using various metal oxides in the pillarization process to enhance surface properties and acidity characteristics, thereby improving the catalytic performance of bentonite for the synthesis of diethyl ether. This development could lead to more efficient, environmentally friendly synthesis processes, aligning with sustainable energy goals.

**Key words** bentonite, pillared bentonite, solid acid catalyst, ethanol dehydration, diethyl ether.

### 1. Introduction

The global economy is expanding quickly, which means a growing need for fuel and energy.<sup>1)</sup> Currently, fuel energy reserves are diminishing yearly and producing emissions that pollute the environment, such as NO<sub>x</sub> and CO<sub>x</sub> gases. This condition provides opportunities for producing environmentally friendly energy.<sup>2,3)</sup> Diethyl ether is an oxygenated fuel that produces lower NO<sub>x</sub> and CO<sub>x</sub> gas emissions during combustion processes than conventional fuels, making it a potential environmentally friendly renewable energy source

to replace fossil fuels.<sup>2,4-6)</sup> As a renewable energy source, diethyl ether is an additive in gasoline and diesel fuels because of its characteristics, such as high volatility, low flash point, octane number greater than 110, high oxygen content, wide ignition limits, low ignition energy, high miscibility with diesel and bioethanol fuels, and low carbon monoxide emissions.<sup>5,7-11)</sup> Physically, diethyl ether has distinct characteristics compared to diesel fuel. Diethyl ether yields higher thermal efficiency than diesel fuel, produces no smoke, and reduces engine noise, as shown in Table 1. Diethyl ether is also widely used in pharmaceutical, perfume, and petroche-

<sup>†</sup>Corresponding author

E-Mail : [karnawijaya@ugm.ac.id](mailto:karnawijaya@ugm.ac.id) (K. Wijaya, UGM)

© Materials Research Society of Korea, All rights reserved.

This is an Open-Access article distributed under the terms of the Creative Commons Attribution Non-Commercial License (<http://creativecommons.org/licenses/by-nc/3.0>) which permits unrestricted non-commercial use, distribution, and reproduction in any medium, provided the original work is properly cited.

mical fields.<sup>12,13)</sup> It is a solvent for organic compounds, such as oils, fats, latex, micro cellulose, and alkaloids.<sup>10,14)</sup>

Diethyl ether is synthesized using a strong homogeneous acid catalyst like sulfuric acid (H<sub>2</sub>SO<sub>4</sub>) or phosphoric acid (H<sub>3</sub>PO<sub>4</sub>) via the ethanol dehydration process, known as the Barbet process.<sup>17)</sup> The main disadvantages of the homogeneous acid catalytic process are the production of very corrosive waste streams and the challenge of removing the products from the catalyst. Nowadays, heterogeneous acid catalysts are being developed as an alternative to accelerate the dehydration reactions of ethanol. Heterogeneous acid catalysts have a different phase from the reactant phase. The advantages of heterogeneous acid catalysts over homogeneous catalysts include ease of separation, non-corrosiveness, non-toxicity, cost-effective purification, and environmental friendliness.<sup>18)</sup> Various heterogeneous acid catalysts for diethyl ether formation have been reported, including metal oxides, zeolites, alumina, silica-alumina, supported phosphoric acid, and hetero-polyacid catalysts. Previous researchers have yet to extensively explore using bentonite-based materials as heterogeneous catalysts in producing ether-based fuels, providing an opportunity for further investigation.

Bentonite is a naturally occurring alumina silicate-based material that holds potential as a catalyst in synthesizing diethyl ether through the ethanol dehydration reaction due to its specific properties and structure, high natural abundance, ease of acquisition, and cost-effectiveness.<sup>19,20)</sup> Bentonite possesses unique physicochemical characteristics, such as good adsorption capacity for both inorganic and organic

substances, large specific surface area, high porosity, and high cation exchange capacity.<sup>21-27)</sup> It also has expandable interlayer spaces, high acidity, and pore sizes that can be modified into micropores and mesopores.<sup>26)</sup>

Pillared bentonite is a promising choice for catalyst support, given its molecular sieve properties and ability to resist sheet deformation even at elevated temperatures.<sup>28)</sup> Pillarization is one of the techniques for modifying clay to enhance catalytic activity and thermal stability in bentonite. The pillarization method involves the intercalation of polyhydroxy cations into the bentonite structure, followed by high-temperature calcination to produce microporous and mesoporous materials that are thermally stable and capable of maintaining their layered structure. As a result of the swelling ability and high cation exchange capacity of bentonite, the basal spacing and specific surface area of pillared bentonite are greater than those of non-pillared bentonite. Therefore, pillared bentonite is widely applicable in catalysis and adsorption.<sup>26)</sup>

In the past decade, pillared bentonite has emerged as a promising catalyst material due to its low cost, high catalytic activity, resistance to leaching, and environmental friendliness,<sup>29,30)</sup> including acetic acid esterification,<sup>31)</sup> CO gas oxidation,<sup>28)</sup> acid-catalyzed hydroxylation of phenol,<sup>32)</sup> transesterification reactions for biodiesel synthesis,<sup>33)</sup> and hydrocracking of fresh and waste cooking oil into biogasoline.<sup>34)</sup> However, fewer studies have used pillared bentonite as a solid catalyst in diethyl ether production.<sup>35,36)</sup> This review briefly discusses the characteristics and properties of bento-

**Table 1.** Comparison of diesel fuel and diethyl ether.<sup>15,16)</sup>

Properties	Diesel	Diethyl ether
Chemical formula	C <sub>13</sub> H <sub>24</sub>	C <sub>4</sub> H <sub>10</sub> O
Density (kg/m <sup>3</sup> )	849	713
Specific gravity	0.83	0.70
Gross calorific value (MJ/kg)	45.5	36.9
Auto-ignition temperature (°C)	210~350	150~160
Cetane number	50	125
Viscosity (mm <sup>2</sup> /s)	3.25	0.23
Stoichiometric air to fuel ratio (kg <sub>air</sub> /kg <sub>fuel</sub> )	14.4	11.2
Boiling point (°C)	180~360	35
Flashpoint (°C)	68	-43
Pour point (°C)	-5	-108
Oxygen content (% by mass)	0	21.6

nite, modifications of bentonite through pillarization, the green synthesis of pillared bentonite, and its performance as a catalyst in synthesizing diethyl ether through ethanol dehydration reactions.

## 2. Structure and Physico-Chemical Properties of Bentonite

Bentonite belongs to the phyllosilicate family and is abundant in nature. Bentonite contains 65–85 % montmorillonite minerals, while the remaining percentage consists of a mixture of impurity minerals such as quartz, cristobalite, feldspar, and other clay minerals. Montmorillonite, a group of alumina silicate minerals, has attracted much attention from researchers because it can be expanded and intercalated with organic and inorganic compounds, forming organic and inorganic composite materials.<sup>22,37,38</sup> The structure of montmorillonite is illustrated in Fig. 1. Bentonite is classified into two types based on its physical properties: sodium bentonite (swelling bentonite), where this type of bentonite has a relatively higher content of  $\text{Na}^+$  cations compared to  $\text{Ca}^{2+}$  and  $\text{Mg}^{2+}$  cations between its layers, and calcium bentonite (non-swelling bentonite), where this type of bentonite has a relatively higher content of  $\text{Ca}^{2+}$  and  $\text{Mg}^{2+}$  cations compared to  $\text{Na}^+$  cations between its layers.

The structure of bentonite has a chemical formula  $\text{M}_x(\text{Al}_{4-x}$

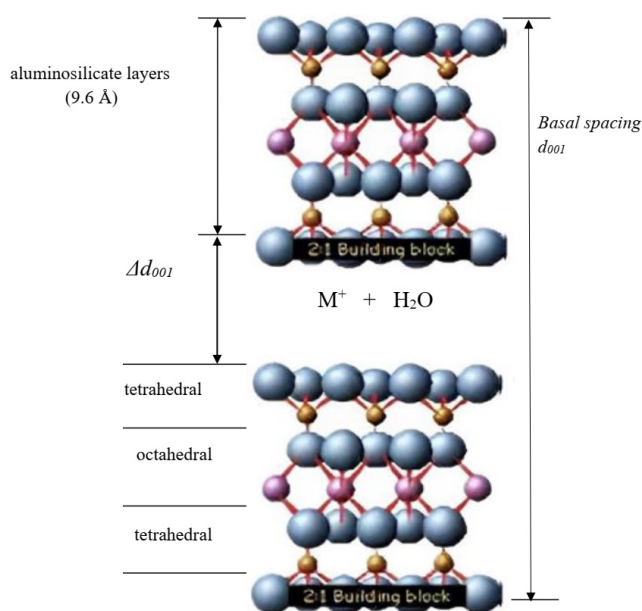


**Fig. 1.** Scheme of montmorillonite. Reprinted from Grim,<sup>41)</sup> Copyright McGraw-Hill 1953.

$\text{Mg}_x\text{Si}_8\text{O}_{20}(\text{OH})_4 \cdot n\text{H}_2\text{O}$  with a 2:1 configuration, consisting of two tetrahedral layers ( $\text{SiO}_4$ ) and one octahedral layer ( $\text{AlO}_4$ ) as the central atom, where oxygen atoms are directly bound to these layers. Electrostatic interactions and hydrogen bonds link tetrahedral-octahedral-tetrahedral layers.<sup>27)</sup> The tetrahedral layer consists of silicon (Si) and oxygen (O) elements, forming  $\text{SiO}_4$ . In contrast, the octahedral layer is occupied by aluminum (Al), oxygen (O), and hydroxyl groups (OH), forming  $\text{AlO}_4(\text{OH})_2$ .<sup>39)</sup> In the tetrahedral layer,  $\text{Si}^{4+}$  can be replaced by  $\text{Al}^{3+}$ , while in the octahedral layer,  $\text{Al}^{3+}$  can be replaced by  $\text{Mg}^{2+}$ . Aluminum atoms can also be substituted by atoms of Fe, Cr, Zr, and other transition metals with significant electronic potential. Additionally, some  $\text{Al}^{3+}$  in the octahedral sheets can be replaced by  $\text{Mg}^{2+}$  without disrupting the structure of the crystal through isomorphic substitution, as illustrated in Fig. 2.<sup>24,40)</sup>

In many minerals, if a positively charged atom with a lower charge replaces an atom with a higher positive charge, it results in a deficiency of positive charges, or, in other words, an excess of negative charge. The monovalent and divalent cations such as  $\text{Na}^+$ ,  $\text{Ca}^{2+}$ , and  $\text{Mg}^{2+}$  are present in interlayers of bentonite to balance the charge in bentonite. These cations are attracted to clay particles and electrostatically bound to the interlayer surfaces of the clay.

The physical and chemical properties of clay will determine its applications, including chemical composition, nature of the oxygen and hydrogen surface atoms, defect sites, layer charge, and the type of exchangeable cations. The properties of clay minerals are classified into (i) clay mineral-water interaction to determine swelling capacity, (ii) CEC (cation exchange capacity), (iii) acidity of clay, (iv) porous structure, (v) gas penetrability, and (vi) ion diffusivity.<sup>27)</sup>

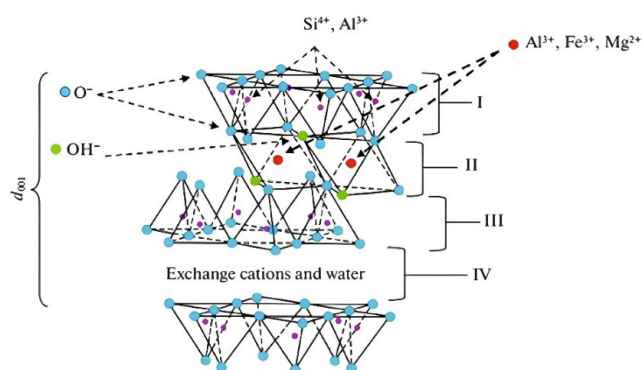


**Fig. 2.** Model structure of bentonite. Reprinted from Vezentsev et al.,<sup>42)</sup> Copyright Springer 2022.

Bentonite is one of the clay mineral groups belonging to the smectite. Smectite exhibits the highest specific surface area and cation exchange capacity (800 m<sup>2</sup>/g and 80~150 meq/100 g) compared to illite (30 m<sup>2</sup>/g and 10~40 meq/100 g), kaolinite (15 m<sup>2</sup>/g and 1~10 meq/100 g), and chlorite (15 m<sup>2</sup>/g and <10 meq/100 g).<sup>43)</sup> Bentonite is an ideal host because bentonite has a good swelling ability and a high cation exchange capacity. Therefore, bentonite can primarily accommodate cations in the interlayer space through a cation exchange mechanism.<sup>22)</sup> The swelling phenomenon increases the interlayer distance after the hydration process. The structure of the bentonite layer will collapse after the dehydration process. We can overcome porosity instability in the bentonite layer structure by the preparation a stable pillar into the interlayer of bentonite with the high pore volume.<sup>27)</sup> However, as shown in Fig. 3, the pillared bentonite can maintain porosity during hydration and dehydration.

Although bentonite has many advantages for application as an adsorbent, catalyst, or ion exchanger, it has one major disadvantage: the distance between bentonite layers expands during the hydration process, but the distance between layers decreases when the dehydration process or heating process, resulting in bentonite with minor permanent micro-porosity and the interlayer surface cannot be used in a chemical reaction. Castro et al.<sup>45)</sup> investigated the catalytic performance of bentonite and Al-pillared bentonite for n-decane hydroconversion reaction. The bentonite has a specific surface area ( $S_{\text{BET}}$ ) of 39 m<sup>2</sup>/g and a total acidity of 56 μmol/g. These values increase after modification of bentonite through pillaring with aluminum metal, with a specific surface area ( $S_{\text{BET}}$ ) of 120 m<sup>2</sup>/g and total acidity of 138 μmol/g. They found that the low surface area and low acidity of bentonite limited the

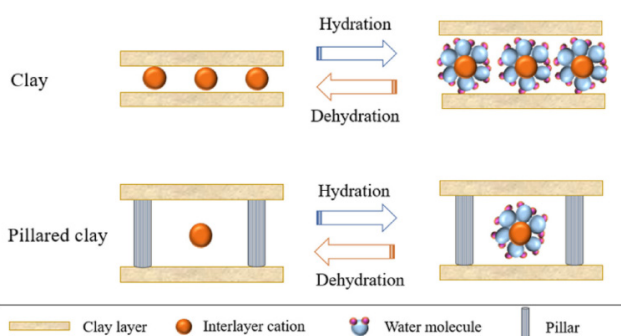


**Fig. 3.** Schematic of raw and pillared clay during hydration and dehydration processes. Reprinted from Najafi et al.,<sup>44)</sup> Copyright Elsevier 2021.

active sites available for catalysis, resulting in lower conversion rates than Al-pillared bentonite. Research by AlSawalha et al.<sup>46)</sup> focused on the acidic properties of various Jordanian clays, including bentonite, kaolinite, and diatomite, for conversion 2-methyl-3-butyn-2-ol (MBOH). The maximum NH<sub>3</sub> desorption rate from the zeolite surface is the highest and decreases from bentonite to kaolinite and diatomite. Bentonite exhibited significantly lower acidity compared to solid acid catalysts like zeolite. This study provides evidence of bentonite's limited surface acidity, affecting its catalytic performance in converting MBOH. The zeolite catalytic activity obtained the highest conversion and the lowest for diatomite. This result leads to the conclusion that the amount of acid sites that can convert MBOH increases with the Si/Al ratio and coincides with the sequence found by NH<sub>3</sub>-TPD. The thermogravimetric analysis data showed that the Ca-bentonite lost adsorbed and hydrated water up to 300 °C, dehydroxylation took place between 300 and 750 °C, and then the 2:1 layer structure completely collapsed above 900 °C, consequently rupturing the clay structure. This structure rupture could cause morphology changes in the bentonite minerals supported by decreased surface area at high temperatures.<sup>47)</sup> However, if bentonite is heated at a high temperature (<600 °C), it will cause the dealumination of bentonite, resulting in a decrease in crystallinity and specific surface area in the bentonite structure.<sup>27)</sup> This limitation restricts bentonite's use as a catalyst for high-temperature reactions, such as hydrocracking or pyrolysis.

Researchers have developed several modification techniques to enhance the catalytic activity of bentonite, including chemical activation using acids, bases, acidic and basic salts, thermal treatment, polymers, and surfactants modification, and pillaring using various metal polyhydroxy cations.<sup>27)</sup> Modified bentonite can be used as a catalyst material or support in various catalytic processes.

### 3. The Bentonite Modification Using the Pillarization Method

Pillarization is the modification technique of bentonite structure to enhance the properties of bentonite by introducing pillar agents between interlayer space, thereby increasing its the surface area, porosity, thermal stability, and surface acidity.<sup>48)</sup> The pillaring process involves the intercala-

tion process of pillaring agents in the form of polyhydroxy metal cations into the silica interlayer in the bentonite structure to produce metal oxides that can support the silicate layers through calcination process,<sup>49,50</sup> as represented in Fig. 4. Therefore, the mechanism of pillar linkage into the interlayer space of clay minerals needs to be clarified.

In the 1990s, acid-activated bentonite began to be used as a precursor in the synthesis of pillared bentonite.<sup>27</sup> However, metal polyhydroxy cations are currently widely used in the pillaring process. Metal polyhydroxy cation-pillared bentonites, such as Al, Ti, and Fe, show higher thermal stability than organic cation-pillared bentonites.<sup>26</sup> Several metals have been investigated for their potential as pillar agents, such as Al-PILC,<sup>28,31,49</sup> Zr-PILC,<sup>14,26,34,46,51-54</sup> Ti-PILC,<sup>45,49,56</sup> Mo-PILC,<sup>57</sup> and Cr-PILC.<sup>30,58</sup> In current developments, researchers are beginning to explore the use of combined metal oxide pillars to enhance surface properties and acidity in bentonite, including Al/Zr-PILC,<sup>19,45</sup> Al/Fe-PILC,<sup>47,59</sup> Al/Co-PILC,<sup>22</sup> Al/Cr-PILC,<sup>30</sup> Al/Fe/Ni-PILC,<sup>60</sup> Fe/Cr-PILC,<sup>58</sup> Ni/Zr-PILC,<sup>61</sup> Mg/Al-PILC.<sup>62</sup>

The pillarization process of bentonite starts with intercalation through the ion exchange of  $\text{Na}^+$ ,  $\text{K}^+$ , or  $\text{Ca}^{2+}$  ions by pillar agents in the form of metal polyhydroxy cations (Al, Zr, Ti, Fe, and Cr) into the interlayer of bentonite structure.<sup>63</sup> The intercalated polycations increase the basal spacing of the bentonites. The metal ions such as  $\text{Al}^{3+}$ ,  $\text{Zr}^{4+}$ ,  $\text{Cr}^{3+}$ , and  $\text{Fe}^{3+}$  are added to a basic solution ( $\text{Na}_2\text{CO}_3$  or  $\text{NaOH}$ ). They stirred at a specific temperature for 3–12 h, then aged at 60–80 °C for 6–24 h to produce metal hydroxy cations as a pillaring agent solution. Then, the pillaring agent solution is slowly added to a bentonite suspension (2 wt%).<sup>64-66</sup> The number of pillars intercalated in the bentonite interlayer depends on the intercalated species cation exchange capacity, charge, and size. In the calcination process, intercalated clay is heated at a temperature ranging from 300–700 °C for a specified time.

In this stage, the metal polyhydroxy cations will dehydrate and dehydroxylate to form the metal oxide pillars. The metal oxide pillars yield temperature stability that permanently keeps the layers apart, preventing collapse. The metal oxide acts as a pillar that opens and supports the bentonite interlayer, resulting in permanent micro-porosity of bentonite. The calcination temperature determines the pore size of pillared clays. The previous research indicated that a high temperature (>700 °C) causes the microporous structure to collapse. On the other hand, pillared clays calcined at 400–600 °C exhibit the characteristics of bidimensional molecular sieves that facilitate the formation of stable pillars and optimize the material's catalytic performance.<sup>44</sup>

The calcination process-induced elimination of protons from the -OH groups of the silicate layer create a bond between the pillar of oxygen and  $\text{Al}^{3+}$  cations in the octahedral sheet.<sup>27</sup> The properties of pillared bentonite materials are affected by metallic cations, clay mineral type, aging time, temperature, and washing and drying methods.<sup>30</sup> Another crucial factor in pillared bentonite synthesis is the calcination temperature, where the heating temperature, duration, and heating rate significantly impact the properties of pillared bentonite materials.

#### 4. Pillared Bentonite: Enhancing Surface Properties and Acidity

Pillarization is an attempt to improve the physicochemical properties of bentonite, including specific surface area, porosity, average pore size, thermal stability, and total acidity, which contribute to the application of bentonite as both catalyst and adsorbent.<sup>55,67</sup> The pillarization process also enhances surface acidity regarding the quantity and strength of Lewis acid and Brønsted acid sites. The hydroxyl groups of silanol groups generate Brønsted acidity in pillared bento-

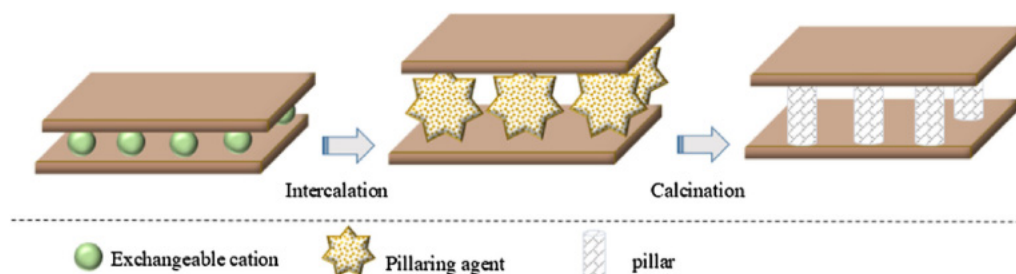


**Fig. 4.** Pillarization of bentonite mechanism. Reprinted from Najafi et al.,<sup>44</sup> Copyright Elsevier 2021.

nite within the layered structure of bentonite. In contrast, Lewis acidity originates from the metal oxide pillars as acceptors of free electron pairs. Pillared bentonite has a higher surface area, porosity, surface acidity (Lewis and Brønsted acid sites), and thermal stability than non-pillared bentonite due to metal oxide pillars supporting the interlayer structure of bentonite.<sup>32,68,69</sup> These properties support the enhanced performance of pillared bentonite as a catalyst compared to non-pillared bentonite in various catalyzed reactions.

Rachmat et al.<sup>70</sup> achieved the pillaring of bentonite using zirconium metal oxide as a solid catalyst for the esterification reaction of lauric acid, resulting in ethanol conversion of 90 %. This high conversion is due to the high acidity of zirconium oxide. Additionally, Khairina et al.<sup>71</sup> conducted pillarization using other metal oxides such as titanium, zirconium, and chromium. The outcomes revealed a substantial increase in surface area from 24.47 m<sup>2</sup>/g to over 150 m<sup>2</sup>/g in pillared bentonite structure. Furthermore, the total acidity of the raw bentonite also increases after the pillarization process. The same results were also reported by Rinaldi et al.<sup>72</sup> who synthesized pillared bentonite using ZrO<sub>2</sub>. The catalyst acidity was determined through NH<sub>3</sub>-TPD analysis. The acidity of bentonite, Zr/PILC, and Ti/PILC was 0.08 mmol/g, 0.55 mmol/g, and 0.26 mmol/g, respectively. The presence of Zr and Ti oxides in bentonite structure as Lewis acid can enhance the acidity of the catalyst due to metal pillaring agents such as titanium, zirconium, and chromium can form connections between the metals and the alumina-silicate bentonite layer.<sup>73</sup> Agustian et al.<sup>74</sup> successfully synthesized pillared bentonite using Ti, Zr, and a combination of Ti/Zr. The resulting pillared bentonite catalyst has a pore structure with high surface area, acidity, and good catalytic performance. The catalysts exhibit a two-to seven-fold increase in specific surface area and expanded basal spacing. The morphology of the catalyst surfaces undergoes significant changes, resulting in smaller pore sizes and higher total acidity than raw bentonite. The acidity of the Ti/Zr-PILC catalyst ranges from 949 to 1,117 μmol/g, and its surface area is between 158 and 169 m<sup>2</sup>/g.

Wijaya et al.<sup>34</sup> studied the preparation of ZrO<sub>2</sub>/SO<sub>4</sub> pillared bentonite for converting coconut oil into gasoline via hydrocracking. A gravimetric method involving an ammonia solution determined the catalyst's surface acidity. The acidity of ZrO<sub>2</sub> pillared bentonite was 3.45 ± 0.02 mmol/g. The

sulfation process with various sulfuric acid solutions of 0.1 to 1 M caused the acidity of ZrO<sub>2</sub> pillared bentonite to increase, and the BZ 1 catalyst (H<sub>2</sub>SO<sub>4</sub> 1 M) was the catalyst with the highest acidity of 5.02 ± 0.04 mmol/g. Liu et al.<sup>24</sup> conducted an acidity test on a tin-exchanged montmorillonite catalyst using the gravimetric method with pyridine solution and NH<sub>3</sub>-TPD. Due to the intercalation of tin ions into the montmorillonite layers, the overall acidity increased significantly, ranging from 0.63 to 0.78 mmol NH<sub>3</sub>/g catalyst. The total acidity on the tin-exchanged montmorillonite gradually decreased as calcination temperatures risen from 300 to 500 °C.

The acid activation process enhances the physicochemical characteristics of pillared bentonite. Research by Mokaya and Jones<sup>75</sup> indicates that acid activation of bentonite before alumina pillaring increases basal spacing to 19.3 Å. After calcination at 500 °C, surface area ranging from 315 to 374 m<sup>2</sup>/g, total pore volume of 0.33~0.48 cm<sup>3</sup>/g, average pore diameter, and surface acidity. A similar phenomenon is also observed in the work of Mokaya and Jones.<sup>76</sup> Whether acid-activated clay is a suitable host for alumina pillaring depends on the extent of clay damage during the acid activation process. This damage causes dealumination in the clay's structure, leading to the formation of a mesoporous structure.

## 5. The Green Synthesis of Pillared Bentonite

Pillared bentonite materials were synthesized by Barrer and MacLeod using organic cations in 1955. Although these cations could be easily intercalated, the resulting products needed improvement, such as weaker interactions between the pillar species and the bentonite layers. This weakness led the pillar species to exchange reactions with more vital species, and the thermal stability was limited to temperatures around 250 °C.<sup>77</sup> In the 1970s, Brindley and Sempels<sup>78</sup> reported using inorganic polycations to synthesize pillared bentonite due to their higher thermal stability.

In general, the synthesis of Al<sub>2</sub>O<sub>3</sub>-pillared bentonite typically begins with the formation of a pillaring solution, namely the Keggin ion ([AlO<sub>4</sub>Al<sub>12</sub>(OH)<sub>24</sub>(H<sub>2</sub>O)<sub>12</sub>]<sup>7+</sup>). The Al-pillaring solution can be synthesized using four methods: (i) hydrolysis of Al<sup>3+</sup> salt (usually AlCl<sub>3</sub>) with NaOH, (ii) hydrolysis of Al<sup>3+</sup> salt (usually AlCl<sub>3</sub>) with Na<sub>2</sub>CO<sub>3</sub>, (iii) electrolysis of AlCl<sub>3</sub>, and (iv) dissolution of aluminum



metal in HCl. Previous researchers have synthesized  $\text{Al}_2\text{O}_3$ -pillared bentonite using a base-hydrolyzed aluminum salt solution.<sup>24,45,79-82)</sup>

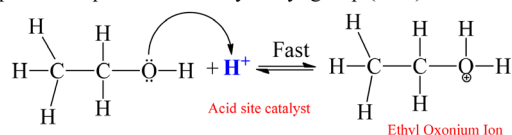
Researchers have begun developing new synthesis methods for the intercalation and pillaring bentonite to reduce synthesis time and water usage. The simple method for synthesizing pillared bentonite has been created using single or combined metal pillaring agents, including ultrasonication,<sup>73,83)</sup> microwave radiation,<sup>84)</sup> and a combination of both methods, as well as one-step high-temperature methods<sup>85)</sup> to reduce synthesis time and friendless. Ultrasonic and microwave radiation methods are suitable for reducing contact time between bentonite and pillaring agents during the intercalation process, allowing ultrasonic synthesis to take only a few minutes.<sup>86)</sup> However, it produces  $\text{Al}_2\text{O}_3$ -pillared bentonite with higher thermal stability and surface characteristics than conventional methods for 24 h. Several studies show that using ultrasonic and microwave radiation methods in synthesizing pillared bentonite reduces water usage by 70–95 % and synthesis time by 70–93 %.<sup>30,87,88)</sup> These parameters make ultrasonic and microwave radiation methods promising as environmentally friendly synthesis methods because they apply principles of green chemistry, such as faster synthesis times, lower energy consumption, and reduced water usage.<sup>89)</sup>

## 6. The Potency of Pillared Bentonite on Diethyl Ether Production

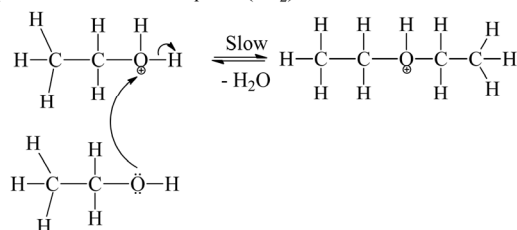
Products resulting from catalytic ethanol dehydration, with higher value-added compared to ethanol, such as hydrogen, diethyl ether, ethylene, 1-butanol, and aldehydes, have been extensively researched due to their sustainability. In general, the schematic reaction of transforming ethanol into diethyl ether can be seen in Fig. 5. The reaction mechanism of ethanol dehydration into diethyl ether using an acid cata-

lyst is shown in Fig. 6. It is generally believed that diethyl ether is formed through a nucleophilic substitution reaction, in which the ethoxy group acts as a nucleophilic reagent and interacts with another ethanol molecule to increase the electrophilicity of the alcohol carbon atom, and further nucleophilic substitution to form diethyl ether (reversible reaction).<sup>90)</sup> A key factor influencing the catalytic activity of pillared bentonite in the ethanol dehydration to diethyl ether is the nature of the surface acidity on the catalyst (Lewis acid sites and Brønsted acid sites).<sup>91,92)</sup> Brønsted acid sites exhibit higher catalytic activity in the ethanol dehydration reaction compared to Lewis acid sites.<sup>36,93)</sup> Świąż et al.<sup>94)</sup> reported that weak acid sites (Lewis acid sites) play a significant role in

Step 1 : Acid protonates the hydroxyl group (-OH)



Step 2 : Substitution Nucleophilic ( $\text{S}_{\text{N}}2$ )



Step 3 : Deprotonation

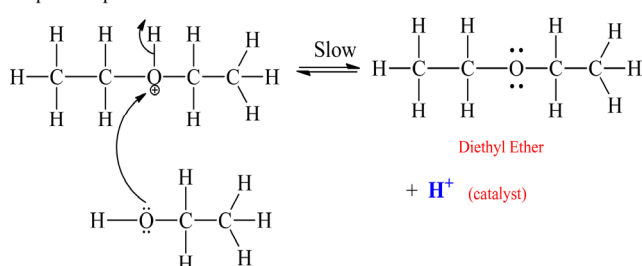


**Fig. 6.** The reaction mechanism of ethanol dehydration using acid catalyst.

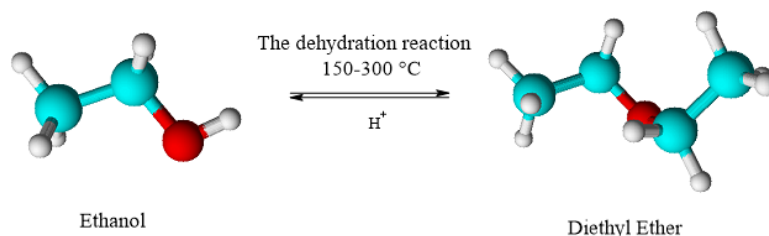


**Fig. 5.** The schematic reaction of transforming ethanol into diethyl ether.

ethanol dehydration to diethyl ether. At the same time, alcohol oligomerization to long-chain hydrocarbons occur at strong acid sites (Brønsted acid sites). High selectivity and conversion of products are determined by weak acid sites (Lewis acid sites) and reduction of strong acid sites (Brønsted acid sites).<sup>2)</sup>

Pillared bentonite, an alumina silicate-based material, shows promise as a catalyst in diethyl ether synthesis. The main characteristics of this catalyst include a high surface acidity, good thermal and hydrothermal stability, a high surface area, and high porosity. There are two possible sources of acidity in pillared bentonite: Brønsted acid sites, which are formed by the hydroxyl groups of silanol groups in the bentonite layer structure, and Lewis acid sites, which are produced by the presence of metal oxide pillars. These metal oxides have vacant orbitals that can accept lone pairs of electrons from other atoms. The summary of the use of pillared bentonite as a catalyst in ether production, diisopropyl ether and dimethyl ether, is listed in Table 2.

Hasanudin et al.<sup>57)</sup> investigated the synthesis of diisopropyl ether through the dehydration reaction of isopropyl alcohol using molybdenum phosphide pillared bentonite (MoP-PILC). Heterogeneous catalyst types, like MoP-PILC, have been reported to possess a high surface area with dominant active Mo sites on the catalyst surface as proton acceptors.<sup>97)</sup> MoP is more stable than other metals and has been utilized in various catalytic reactions with good cycle resistance. The intercalation of Mo metal into the Na-bentonite silica framework will enhance bentonite's pore surface area, pore volume, and pore diameter. The acidity after pillaring also expanded due to MoP-PILC having more Lewis acid sites and a larger pore than Na-bentonite. MoP-PILC 4 meq/g has the highest acidity from 1.5755–5.7732 mmol/g, indicating the increase of the catalytic activity. The catalytic

activity is affected by the site acid's surface concentration and the acid's strength. The optimum composition of the MoP-PILC catalyst yielding the highest diisopropyl ether yield of 64.5 % is at 4 meq/g. This result is attributed to the intercalation of Mo metal into MoP-PILC, which possesses half-filled d orbitals as Lewis acid sites, playing a crucial role in the isopropyl alcohol dehydration reaction and enhancing diisopropyl ether.<sup>98)</sup>

A similar study was conducted by Hasanudin et al.<sup>95)</sup> using zirconium phosphate pillared Na-montmorillonite as the catalyst. This catalyst achieved a methanol conversion rate of 96.76 %, a dimethyl ether product yield of 96.8 %, and a dimethyl ether selectivity of 93.67 % over a temperature range of 150–350 °C, with an LSHV (liquid space hourly velocity) of 2.54 h<sup>-1</sup> using N<sub>2</sub> gas flow. These outcomes can be attributed to the presence of acidic hydrogen ions and the presence of moderate to strong acid sites, which directly impact the catalyst's performance in methanol dehydration. According to Gao et al.<sup>99)</sup> zirconium phosphate can improve reactant diffusion and minimize the formation of side products. The synthesis of diethyl ether through the ethanol dehydration reaction using an alumina-intercalated vermiculite catalyst was conducted by Marosz et al.<sup>96)</sup> over a temperature range of 50 to 300 °C. As the temperature increased, the ethanol conversion rate increased, reaching its maximum of 98 % under optimal conditions at 300 °C with the alumina-pillared catalyst (Al-PILC). The Al-PILC catalyst demonstrated the highest selectivity for diethyl ether at 72 %. Nevertheless, as the temperature was further raised, the selectivity shifted toward ethylene while reducing the selectivity for diethyl ether. The dehydration of ethanol to diethyl ether is an exothermic process and is more favorable at lower temperatures.<sup>100)</sup>

At elevated temperatures, ethanol dehydration tends to

**Table 2.** Summary of pillared bentonite as a catalyst in ether production.

Catalyst	Feedstock	Reaction condition	Ether yield	Reference
MoP-PILC	Isopropyl alcohol	T <sup>1)</sup> : 160 °C W <sup>2)</sup> : 2 g, 4 g, 6 g, dan 8 g	Diisopropyl ether 64.5 %	Sabre et al. <sup>56)</sup>
ZrP-PILC	Methanol	T: 150–350 °C W: 1 g	Dimethyl ether 93.6 %	Hasanudin et al. <sup>95)</sup>
Al-PILC	Ethanol	T: 150–350 °C W: 0.1 g	Diethyl ether 72 %	Marosz et al. <sup>96)</sup>

<sup>1)</sup>T, reaction temperature; <sup>2)</sup>W, catalyst weight.



shift toward ethylene formation. This change is supported by reduced catalyst selectivity for diethyl ether products as the temperature increases. At 300 °C, ethylene becomes the primary product. Catalytic tests showed that PILC catalysts displayed more excellent activity compared to  $\gamma$ -Al<sub>2</sub>O<sub>3</sub>. While  $\gamma$ -Al<sub>2</sub>O<sub>3</sub> catalysts exhibited high selectivity towards diethyl ether products, their selectivity for ethylene was lower than that of PILC. Based on this data, it can be inferred that  $\gamma$ -Al<sub>2</sub>O<sub>3</sub> is better suited for converting ethanol to DEE, while PILC is more effective in converting ethanol to ethylene. This can be clarified by examining the surface acidity of PILC, which is attributed to the presence of acid sites on the vermiculite surface and alumina oxide used as pillars. Research has shown that the catalytic performance of pillarized bentonite in methanol and ethanol dehydration reactions depends on these acid sites' surface concentration and strength.

Another factor influencing the yield and selectivity of diethyl ether is the reaction temperature, which typically ranges from 150~350 °C in the process of forming diethyl ether through ethanol dehydration.<sup>101)</sup> Suppose the ethanol dehydration reaction has been carried out at a high temperature (350~500 °C). In this case, the reaction is endothermic.<sup>12)</sup> As a result, the dehydration reaction will yield more ethylene products than diethyl ether products.<sup>102)</sup> The synthesis of diethyl ether via dehydration of ethanol reaction is preferred at low temperatures, and the reaction that occurs is exothermic. As a result, the conversion of ethanol to diethyl ether is more down at low temperatures. Consequently, the reaction requires a catalyst to enhance catalytic activity at low temperatures while maintaining high diethyl ether selectivity.<sup>5)</sup> Besides that, ethanol hydrogenation can produce acetaldehydes as a side reaction.<sup>2)</sup>

## 7. Challenges and Future Perspectives

Fascinatingly, pillarized bentonite exhibits a broad spectrum of surface area and pore structure, and the surface acidity can be altered by changing the type of pillarizing agent employed during the pillarization process. Each pillarizing agent offers unique benefits and distinct material properties, making it suitable for various applications. Pillared bentonite materials possess unique characteristics such as high surface acidity, surface area, porosity, and thermal

stability. However, the yield and selectivity of diethyl ether produced are still low (<80 %), and previous research on the application of pillared bentonite as a diethyl ether catalyst has received limited attention and remains underreported. However, some challenges still restrict further development, such as superior catalyst acidity and high product selectivity. These challenges may provide new research opportunities and directions for developing high-surface acidity pillared bentonite materials for increased product yield and catalyst selectivity.

The catalytic activity of pillared bentonite in the ethanol dehydration reaction to diethyl ether production depends on surface properties and the surface concentration and strength of acid sites (both Brønsted and Lewis acid sites). Additional research is required to enhance the catalytic performance of pillarized bentonite. This could involve incorporating one or two transition metals, such as Ti, Co, Ni, Mo, and Zr, and activation with strong acids like H<sub>2</sub>SO<sub>4</sub> or H<sub>3</sub>PO<sub>4</sub>. This approach is expected to enhance the surface characteristics of bentonite, including surface area, porosity, and surface acidity.

## 8. Conclusion

The comprehensive review explores pillared bentonite's capabilities in synthesizing diethyl ether, an environmentally friendly fuel alternative. It highlights the inherent properties of bentonite, such as its high cation exchange capacity and porosity, which is enhanced by pillarization. This modification involves intercalating polyhydroxy cations into bentonite's structure, improving its thermal stability and catalytic efficiency. Pillared bentonite is a promising material due to its environmental friendliness, cost-effectiveness, and ability to modify its surface properties and acidity, making it suitable as a heterogeneous acid catalyst in producing diethyl ether from ethanol dehydration. Despite the potential of pillared bentonite, several challenges limit its widespread application, primarily concerning optimizing catalyst yield and selectivity for diethyl ether production. The review suggests that future research should focus on using various metal oxides for pillarization to enhance bentonite's surface characteristics, acidity properties, and catalytic performance for synthesizing diethyl ether. The research could include exploring new synthesis methods, like ultrasonication and

microwave radiation, which could decrease environmental impact and increase efficiency. The development of pillared bentonite with higher surface acidity and better pore structure may lead to improved outcomes in diethyl ether synthesis, contributing to the broader use of renewable energy sources.

## Acknowledgement

This work was supported by Penelitian Disertasi Doktor (PDD), Project of Ministry of Education, Culture, Research, and Technology (Kemdikbudristek) Indonesia 2023 under Contract Number 122/E5/PG.02.00.PL/2023;3104/UN1/DIT LIT/Dit-Lit/PT.01.03/2023.

## References

1. S. Zeng, J. Li, N. Wang, W. Zhang, Y. Wei, Z. Liu and S. Xu, *Energy Fuels*, **35**, 12319 (2021).
2. C. Autthanit, N. Likitpiriya, P. Praserttham and B. Jongsomjit, *ACS Omega*, **6**, 19911 (2021).
3. A. S. Silitonga, T. M. I. Mahlia, H. C. Ong, T. M. I. Riayatsyah, F. Kusumo, H. Ibrahim, S. Dharma and D. Gumilang, *Energy Sources, Part A*, **39**, 2006 (2017).
4. C. E. Guzmán-Martínez, R. Maya-Yescas, A. J. Castro-Montoya and F. Nápoles Rivera, *Chem. Eng. Process.*, **159**, 108238 (2021).
5. T. K. R. de Oliveira, M. Rosset and O. W. Perez-Lopez, *Catal. Commun.*, **104**, 32 (2018).
6. K. Wijaya, A. Nadia, A. Dinana, A. F. Pratiwi, A. D. Tikoalu and A. C. Wibowo, *Catalysts*, **11**, 1150 (2021).
7. J. Abu-Dahrieh, D. Rooney, A. Goguet and Y. Saih, *Chem. Eng. J.*, **203**, 201 (2012).
8. S. Lee and T. Y. Kim, *Appl. Therm. Eng.*, **121**, 454 (2017).
9. H. Venu and V. Madhavan, *Fuel*, **189**, 377 (2017).
10. R. Alviyani, A. Wahyudi, I. Gunardi, A. Roesyadi, F. Kurniawansyah and D. Hari Prajitno, *MATEC Web Conf.*, **156**, 06003 (2018).
11. A. Singh and S. Singh, *J. Inst. Eng. (India): Ser. C*, **102**, 705 (2021).
12. T. K. Phung and G. Busca, *Chem. Eng. J.*, **272**, 92 (2015).
13. Ł. Kuterasiński, U. Filek, M. Zimowska, B. D. Napruszewska, M. Gackowski and P. J. Jodłowski, *Mater. Res. Bull.*, **147**, 111652 (2022).
14. M. J. Marbun, F. Kurniawansyah, D. H. Prajitno and A. Roesyadi, *IOP Conf. Ser.: Mater. Sci. Eng.*, **543**, 012058 (2019).
15. E. Christensen, A. Williams, S. Paul, S. Burton and R. L. McCormick, *Energy Fuels*, **25**, 5422 (2011).
16. A. Ibrahim, *Appl. Therm. Eng.*, **107**, 853 (2016).
17. I. A. Muna, F. Kurniawansyah, M. Mahfud and A. Roesyadi, *AIP Conf. Proc.*, **2349**, 020041 (2021).
18. A. Aneu, R. A. Pratika, Hasanudin, S. Gea, K. Wijaya and W. C. Oh, *Silicon*, **15**, 5037 (2023).
19. S. J. Baloyi and J. A. Moma, *J. Environ. Chem. Eng.*, **8**, 104186 (2020).
20. R. R. Elmorsi, G. A. H. Mostafa and K. S. Abou-El-Sherbini, *J. Environ. Chem. Eng.*, **9**, 104606 (2021).
21. M. Segad, S. Hanski, U. Olsson, J. Ruokolainen, T. Åkesson and B. Jönsson, *J. Phys. Chem. B*, **116**, 7596 (2012).
22. F. Bertella and S. B. C. Pergher, *Microporous Mesoporous Mater.*, **201**, 116 (2015).
23. M. K. Uddin, *Chem. Eng. J.*, **308**, 438 (2017).
24. J. Liu, X. Q. Wang, B. B. Yang, C. L. Liu, C. L. Xu and W. S. Dong, *Renewable Energy*, **120**, 231 (2018).
25. P. Belousov, A. Semenkova, T. Egorova, A. Romanchuk, S. Zakusin, O. Dorzhieva, E. Tyupina, Y. Izosimova, I. Tolpeshta, M. Chernov and V. Krupskaya, *Minerals*, **9**, 625 (2019).
26. N. Ayub and M. N. Chaudhry, *Pol. J. Environ. Stud.*, **30**, 1039 (2021).
27. S. Barakan and V. Aghazadeh, *Environ. Sci. Pollut. Res.*, **28**, 2572 (2021).
28. F. T. Basoglu and S. Balci, *J. Mol. Struct.*, **1106**, 382 (2016).
29. F. Tomul, *J. Nanomater.*, **2012**, 237853 (2012).
30. J. Baloyi, T. Ntho and J. Moma, *Catal. Lett.*, **148**, 3655 (2018).
31. P. Wahyuningsih, K. Wijaya, W. Trisunaryanti, A. Mara and Suheryanto, *Asian J. Chem.*, **27**, 1304 (2015).
32. I. Fatimah, *J. Adv. Res.*, **5**, 663 (2014).
33. P. Wahyuningsih, T. Harmawan, R. Fajri and R. A. Putra, in *Proceedings of the 2nd International Conference on Science, Technology, and Modern Society (Langsa, Aceh, November 2020)*. ed. T. M. Ridha Al Auwal, H. Saputra, F. I. Aksa, R. A. Putra and Z. Arico (Atlantis Press, Netherlands, 2021) p.28.
34. K. Wijaya, M. A. Kurniawan, W. D. Saputri, W. Trisunaryanti, M. Mirzan, P. L. Hariani and A. D. Tikoalu, *J. Environ. Chem. Eng.*, **9**, 105399 (2021).
35. W. Alharbi, E. Brown, E. F. Kozhevnikova and I. V. Kozhevnikov, *J. Catal.*, **319**, 174 (2014).
36. T. Kamsuwan, P. Praserttham and B. Jongsomjit, *J. Oleo Sci.*, **66**, 199 (2017).
37. N. D. Hutson, M. J. Hoekstra and R. T. Yang, *Microporous Mesoporous Mater.*, **28**, 447 (1999).
38. A. Gil, L. M. Gandía and M. A. Vicente, *Catal. Rev.: Sci.*

- Eng., **42**, 145 (2000).
39. A. Maged, J. Iqbal, S. Kharbish, I. S. Ismael and A. Bhatnagar, *J. Hazard. Mater.*, **384**, 121320 (2020).
40. H. Rahimzadeh, M. Tabatabaei, M. Aghbashlo, H. K. S. Panahi, A. Rashidi, S. A. H. Goli, M. Mostafaei, M. Ardjmand and A. S. Nizami, *Front. Energy Res.*, **6**, 137 (2018).
41. R. E. Grim, *Clay Mineralogy*, 2nd ed., p.165, McGraw Hill Book Company, New York, USA (1968).
42. A. I. Vezentsev, N. A. Volovicheva, S. V. Korol'kova and P. V. Sokolovskiy, *Russ. J. Phys. Chem. A*, **96**, 381 (2022).
43. B. Karpiński and M. Szkodo, *Adv. Mater. Sci.*, **15**, 37 (2015).
44. H. Najafi, S. Farajfaed, S. Zolgharnian, S. H. Mosavi Mirak, N. Asasian-Kolur and S. Sharifian, *Process Saf. Environ. Prot.*, **147**, 8 (2021).
45. A. Castro, J. Amaya, R. Molina and S. Moreno, *Catal. Today*, **356**, 284 (2020).
46. P. A. Henao-Aguire, I. F. Macías-Quiroga, G. I. Giraldo-Gómez and N. R. Sanabria-González, *Bull. Chem. React. Eng. Catal.*, **16**, 491 (2021).
47. M. Toor, B. Jin, S. Dai and V. Vimonses, *J. Ind. Eng. Chem.*, **21**, 653 (2015).
48. M. Chauhan, V. K. Saini and S. Suthar, *J. Clean. Prod.*, **258**, 120686 (2020).
49. I. P. Okoye and C. Obi, *Res. J. Appl. Sci.*, **6**, 84 (2011).
50. Y. Wang, W. Wang, Y. Chen, J. Ma and R. Li, *Chem. Eng. J.*, **250**, 248 (2014).
51. A. Suseno, Priyono, K. Wijaya and W. Trisunaryanti, *IOP Conf. Ser.: Mater. Sci. Eng.*, **107**, 012040 (2016).
52. M. Muzakky and H. Poernomo, *Indones. J. Chem.*, **18**, 632 (2018).
53. Ruslan, Khairuddin, J. Hardi and M. Mirzan, *AIP Conf. Proc.*, **2243**, 030022 (2020).
54. J. M. Martinez, M. S. Conconi, F. Booth and N. M. Rendtorff, *J. Therm. Anal. Calorim.*, **145**, 51 (2021).
55. M. Chauhan, V. K. Saini and S. Suthar, *J. Hazard. Mater.*, **399**, 122832 (2020).
56. E. V. Sabre, B. M. Viola, A. L. Cánepa and S. G. Casuscelli, *Top. Catal.*, **65**, 1373 (2022).
57. H. Hasanudin, W. R. Asri, K. Tampubolon, F. Riyanti, W. Purwaningrum and K. Wijaya, *Pertanika J. Sci. Technol.*, **30**, 1739 (2022).
58. R. R. Widjaya, N. Saridewi, A. A. Putri, N. Rinaldi and A. A. Dwiatmoko, *IOP Conf. Ser.: Mater. Sci. Eng.*, **1011**, 012008 (2021).
59. M. Said, L. I. Saputri, W. Purwaningrum, F. Riyanti and P. L. Hariani, *J. Phys.: Conf. Ser.*, **1933**, 012114 (2021).
60. T. M. Mudrinić, M. J. Ajduković, N. P. Jović-Jovičić, S. R. Marinović, Z. D. Mojović, A. D. Milutinović-Nikolić and P. T. Banković, *React. Kinet., Mech. Catal.*, **124**, 75 (2018).
61. M. Mirzan, K. Wijaya, I. I. Falah and W. Trisunaryanti, *J. Phys.: Conf. Ser.*, **1242**, 012013 (2019).
62. M. Xia, R. Gao, Y. Wang, S. Wang, Y. Yun and J. Dou, *Environ. Technol.*, **42**, 1652 (2021).
63. B. K. Aziz, D. M. Salh, S. Kaufhold and P. Bertier, *Molecules*, **24**, 2720 (2019).
64. J. Baloyi, T. Ntho and J. Moma, *J. Porous Mater.*, **26**, 583 (2019).
65. A. Olaya, S. Moreno and R. Molina, *Catal. Commun.*, **10**, 697 (2009).
66. A. Olaya, S. Moreno and R. Molina, *Appl. Catal., A*, **370**, 7 (2009).
67. L. Chmielarz, B. Gil, P. Kuśtrowski, Z. Piwowarska, B. Dudek and M. Michalik, *J. Solid State Chem.*, **182**, 1094 (2009).
68. A. Santhana Krishna Kumar, R. Ramachandran, S. Kalidhasan, V. Rajesh and N. Rajesh, *Chem. Eng. J.*, **211-212**, 396 (2012).
69. A. G. Thanos, E. Katsou, S. Malamis, K. Psarras, E. A. Pavlatou and K. J. Haralambous, *Chem. Eng. J.*, **211-212**, 77 (2012).
70. A. Rachmat, W. Trisunaryanti, Sutarno and K. Wijaya, *Mater. Renewable Sustainable Energy*, **6**, 13 (2017).
71. N. N. L. Khairina, A. Kristiani, R. R. Widjaya, E. Agustian, A. A. Dwiatmoko and N. Rinaldi, *AIP Conf. Proc.*, **2493**, 060017 (2022).
72. N. Rinaldi, N. D. E. Purba, A. Kristiani, E. Agustian, R. R. Widjaya and A. A. Dwiatmoko, *Catal. Commun.*, **174**, 106598 (2023).
73. E. Agustian, A. Rachmawati, N. D. E. Purba, N. Rinaldi and A. L. Juwono, *J. Phys.: Conf. Ser.*, **1951**, 012017 (2021).
74. E. Agustian, A. L. Juwono, N. Rinaldi and A. A. Dwiatmoko, *S. Afr. J. Chem. Eng.*, **45**, 228 (2023).
75. R. Mokaya and W. Jones, *J. Catal.*, **153**, 76 (1995).
76. R. Mokaya and W. Jones, *J. Porous Mater.*, **1**, 97 (1995).
77. P. Cool and E. F. Vansant, *Molecular Sieves*, ed. H. G. Karge and J. Weitkamp, p.265, Springer, Berlin, Germany (1998).
78. G. W. Brindley and R. E. Sempels, *Clay Miner.*, **12**, 229 (1977).
79. P. Kumar, R. V. Jasra and S. G. T. Bhat, *Indian J. Chem., Sect. A: Inorg., Phys., Theor. Anal.*, **36**, 667 (1997).
80. A. A. G. Tomlinson, *J. Porous Mater.*, **5**, 259 (1998).
81. M. L. Chávez-García, L. de Pablo-Galán and M. P. Saucedo-Ramírez, *J. Mex. Chem. Soc.*, **50**, 36 (2006).
82. I. Fatimah and K. Wijaya, *ITB J. Sci.*, **43**, 123 (2011).
83. N. Rinaldi and A. Kristiani, *AIP Conf. Proc.*, **1823**, 020063 (2017).
84. B. González, A. H. Pérez, R. Trujillano, A. Gil and M. A.

- Vicente, *Materials*, **10**, 886 (2017).
85. Z. Chen, J. Li, Z. Cheng and S. Zuo, *Appl. Clay Sci.*, **163**, 227 (2018).
86. N. R. Sanabria, R. Molina and S. Moreno, *Catal. Lett.*, **130**, 664 (2009).
87. F. Tomul, *Appl. Clay Sci.*, **120**, 121 (2016).
88. E. Ruiz-Hitzky and P. Aranda, *J. Sol-Gel Sci. Technol.*, **70**, 307 (2014).
89. A. Aneu, K. Wijaya and A. Syoufian, *J. Porous Mater.*, **29**, 1321 (2022).
90. J. Lv, D. Wang, L. Peng, X. Guo, W. Ding and W. Yang, *Catalysts*, **13**, 994 (2023).
91. C. P. Nash, A. Ramanathan, D. A. Ruddy, M. Behl, E. Gjersing, M. Griffin, H. Zhu, B. Subramaniam, J. A. Schaidle and J. E. Hensley, *Appl. Catal., A*, **510**, 110 (2016).
92. M. Viftaria, N. Nurhayati and S. Anita, *J. Phys.: Conf. Ser.*, **1351**, 012040 (2019).
93. A. Khamkeaw, T. Asavamongkolkul, T. Perngyai, B. Jongsomjit and M. Phisalaphong, *Molecules*, **25**, 4063 (2020).
94. A. Świąż, A. Kowalczyk, B. Gil and L. Chmielarz, *RSC Adv.*, **12**, 9395 (2022).
95. H. Hasanudin, W. R. Asri, Q. U. Putri, Z. Fanani, D. Bahrin, T. E. Agustina and K. Wijaya, *Iran. J. Catal.*, **12**, 389 (2022).
96. M. Marosz, A. Kowalczyk and L. Chmielarz, *Catal. Today*, **355**, 466 (2020).
97. M. R. Sun Kou, S. Mendioroz, P. Salerno and V. Muñoz, *Appl. Catal., A*, **240**, 273 (2003).
98. M. C. Alvarez-Galvan, J. M. Campos-Martin and J. L. G. Fierro, *Catalysts*, **9**, 293 (2019).
99. H. Gao, L. Hu, Y. Hu, X. Lv, Y. B. Wu and G. Lu, *Catal. Sci. Technol.*, **11**, 4417 (2021).
100. T. K. Phung, L. Proietti Hernández, A. Lagazzo and G. Busca, *Appl. Catal., A*, **493**, 77 (2015).
101. T. K. Phung, R. Radikapratama, G. Garbarino, A. Lagazzo, P. Riani and G. Busca, *Fuel Process. Technol.*, **137**, 290 (2015).
102. Z. S. B. Sousa, C. O. Veloso, C. A. Henriques and V. Teixeira da Silva, *J. Mol. Catal. A: Chem.*, **422**, 266 (2016).

## Author Information

### Puji Wahyuningsih

Student, Department of Chemistry, Faculty of Mathematics and Natural Sciences, Universitas Gadjah Mada  
Lecturer, Department of Chemistry, Faculty of Engineering, Universitas Samudra

### Karna Wijaya

Professor, Department of Chemistry, Faculty of Mathematics and Natural Sciences, Universitas Gadjah Mada

### Aulia Sukma Hutama

Lecturer, Department of Chemistry, Faculty of Mathematics and Natural Sciences, Universitas Gadjah Mada

### Aldino Javier Saviola

Student, Department of Chemistry, Faculty of Mathematics and Natural Sciences, Universitas Gadjah Mada

### Indra Purnama

Lecturer, Graduate School of Agricultural Sciences, Universitas Lancang Kuning

### Won-Chun Oh

Professor, Department of Advanced Materials and Engineering, Hanseo University

### Muhammad Aziz

Professor, Institute of Industrial Science, The University of Tokyo